Heterogeneous Ozone Oxidation Reactions of 1-Pentene, Cyclopentene, Cyclohexene, and a Menthenol Derivative Studied by Sum Frequency Generation

Grace Y. Stokes, Avram M. Buchbinder, Julianne M. Gibbs-Davis, Karl A. Scheidt, and Franz M. Geiger*

Department of Chemistry, Northwestern University, 2145 Sheridan Road, Evanston, Illinois 60208

Received: April 15, 2008; Revised Manuscript Received: September 11, 2008

We report vibrational sum frequency generation (SFG) spectra of glass surfaces functionalized with 1-pentene, 2-hexene, cyclopentene, cyclohexene, and a menthenol derivative. The heterogeneous reactions of ozone with hydrocarbons covalently linked to oxide surfaces serve as models for studying heterogeneous oxidation of biogenic terpenes adsorbed to mineral aerosol surfaces commonly found in the troposphere. Vibrational SFG is also used to track the C═C double bond oxidation reactions initiated by ozone in real time and to characterize the surface-bound product species. Combined with contact angle measurements carried out before and after ozonolysis, the kinetic and spectroscopic studies presented here suggest reaction pathways involving vibrationally hot Criegee intermediates that compete with pathways that involve thermalized surface species. Kinetic measurements suggest that the rate limiting step in the heterogeneous C═C double bond oxidation reactions is likely to be the formation of the primary ozonide. From the determination of the reactive uptake coefficients, we find that ozone molecules undergo between 100 and 10000 unsuccessful collisions with C═C double bonds before the reaction occurs. The magnitude of the reactive uptake coefficients for the cyclic and linear olefins studied here does not follow the corresponding gas-phase reactivities but rather correlates with the accessibility of the C═C double bonds at the surface.

I. Introduction

According to the 2007 Intergovernmental Panel on Climate Change report, "Anthropogenic contributions to aerosols (primarily sulphate, organic carbon, black carbon, nitrate, and dust)... remain the dominant uncertainty in radiative forcing."[1] Radiative forcing, i.e., the net difference in incoming and outgoing solar radiation of the planet,[2,3] is one of the key parameters in computer models used to evaluate the past and predict the future of Earth's climate. Reducing the uncertainties in radiative forcing should thus allow for more accurate assessments of how human activities impact our environment. Including heterogeneous and multiphase[4] processes in atmospheric models has resolved discrepancies between measured ozone levels and those calculated using gas-phase-only atmospheric models.[5] Therefore, one scientific goal in many fundamental studies of heterogeneous atmospheric chemistry is to reach the high level of scientific understanding that is now established for homogeneous atmospheric reactions by including molecular-level mechanistic information in the atmospheric models.

An important set of heterogeneous reactions involves mineral dust. Dust clouds, which can form over northern Africa, southern Europe, and central Asia,[6−13] can have up to week-long lifetimes and routinely reach the Americas, including the east and west coasts of the continental United States.[14,15] On the local scale, dust clouds can be linked to agricultural activities[13,16−21] and adverse effects on health.[22−24] Mineral dust particles are also implicated in key steps involving the microphysics of aerosol formation[25−28] and are believed to impact global climate by influencing the atmospheric radiative budget on the global scale.[2,3] Characterizing the reactions that influence radiative forcing can be complicated by organic compounds, such as terpenes, found on the surfaces of mineral dust particles.

Terpenes are a class of organic compounds emitted by biogenic sources such as trees; their emissions can outweigh emissions from anthropogenic sources by a factor of 5:1.[3] They are often doubly unsaturated and may become partially oxidized in the gas phase by oxygenation of one olefin moiety.[29,30] After adsorbing to the hydrophilic surfaces of mineral dust through their polar ends, the remaining C═C double bond becomes available for reaction with common atmospheric oxidants such as ozone.

Previous research has shown that heterogeneous reactions between ozone and unsaturated organic compounds commonly found on aerosols are crucial for assessing the impact that aerosols have on the chemical composition of the atmosphere and radiative forcing.[2,3,31−54] To better understand naturally occurring aerosols, many researchers have conducted laboratory experiments over the past decade involving reactions between ozone and surface alkenes as models for heterogeneous atmospheric reactions. Dubowski et al. studied the oxidation of C═C double bond terminated silanes on silicon (with a native oxide layer) by ozone using attenuated total reflectance infrared Fourier transform spectroscopy (ATR-FTIR) at 296 K.[41] Fiegland et al.[38] used reflection−absorption infrared spectroscopy studies to observe the IR signatures of terminal vinyl groups decrease and carbonyl signatures appear upon exposure to ozone. The lifetimes calculated from transformations of surface-bound organic reactants were found to be approximately 20−30 times shorter than those of the corresponding gas-phase olefins, and the authors identified that the reaction followed a Langmuir−Hinshelwood mechanism. Reaction probabilities based on these laboratory experiments varied between 10^{-6} and 10^{-5} for ozone concentrations below approximately 4 ppm. Similar experiments

* To whom correspondence should be addressed. E-mail: geigerf@chem.northwestern.edu. Fax: +847-491-7713.

10.1021/jp803277s CCC: $40.75
Published on Web 10/23/2008

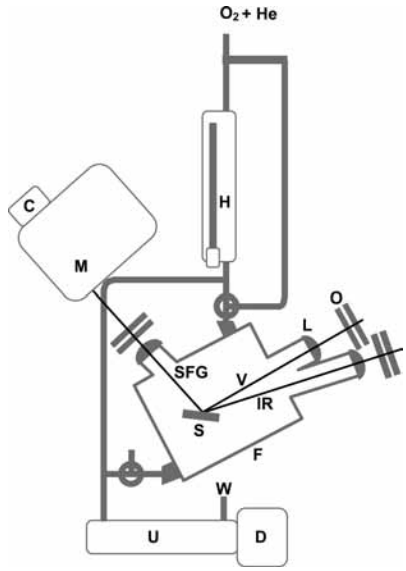

Figure 1. Experimental setup. H = mercury pen ray lamp, U = UV−vis cell, W = waste, D =UV−vis detector, O = visible and IR waveplates and filters, L = lens, V = visible upconverter light field, IR = IR probe light field, SFG = sum frequency light field, S = sample, M = spectrograph, and C = charge coupled device.

were conducted by Moise and Rudich, who monitored the ozonation of surfaces functionalized with aliphatic and vinylic groups.[43] They reported that 0.04 to 4 ppb ozone levels caused vinylic adlayers to exhibit transformations with reactive uptake coefficients between 1×10^{-4} and 3×10^{-4}, while uncoated glass slides and glass slides functionalized with saturated hydrocarbon compounds were found to be much less reactive with coefficients less than 3×10^{-6}. Grassian and co-workers used a Knudsen cell to monitor reactions of ozone with SiO_2 particles functionalized with either octenyltrichlorosilane or octyltrichlorosilane[42] and reported initial reaction probabilities of 7×10^{-5}. Thomas et al. identified CH_2O, CO, and CO_2 as gas-phase products,[44] and ATR-FTIR studies allowed for the direct observation of the decrease in vinylic CH vibrations. Following oxidation, the spectra showed product species containing terminal methyl, carbonyl, and hydrogen-bonded carbonyl groups. Ozone reactions with surface-bound alkenes are typically much faster than expected on the basis of gas-phase kinetics.

While the aforementioned studies show efficient interactions between ozone and atmospherically relevant alkenes, they are limited to a group of commercially available straight chain unsaturated compounds.[32,36,38,41,47−52,55−60] In this work, we expand the scope of models for tropospheric heterogeneous organic oxidation to include the surface chemistry of tailor-made, chemically diverse unsaturated cyclic and straight chain hydrocarbon-modified surfaces. Specifically, we focus on the characterization and interaction of ozone with glass slides that have been functionalized with tailor-made tropospherically relevant hydrocarbons commonly found in continental biogenic emissions, namely, terpenes. We use glass as a proxy for mineral dust because the cores of mineral dust particles are mainly composed of silica and silicate minerals[14,61] and functionalize the glass substrates with atmospherically relevant organic compounds. To address the complexity and diversity of aerosols, we investigate oxide surfaces containing cyclohexene, cyclopentene, a menthenyl derivative, and related olefins, which contain important chemical motifs commonly found in volatile biogenic organic compounds.[2,3,62] We avoid hydrocarbon evaporation from the glass surfaces by using covalent linkers and focus therefore solely on the surface reaction rates when studying time-dependent processes.

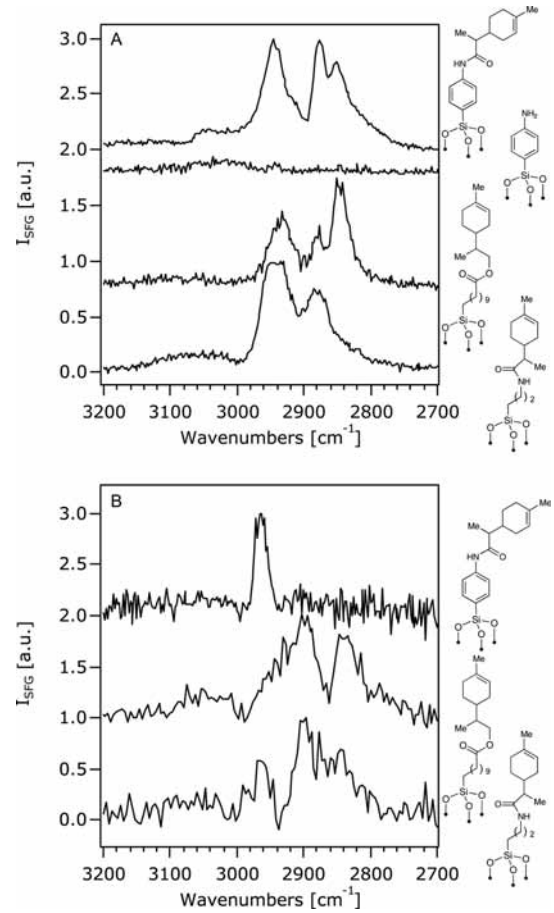

Figure 2. (A) ssp-polarized SFG spectra obtained from (top to bottom) an aniline silane-linked menthenyl-functionalized glass slide, an aniline silane-functionalized glass slide, and decanoic ester- and propylamine-linked menthenyl-functionalized surfaces. (B) sps-polarized SFG spectra obtained from (top to bottom) an aniline silane-linked menthenyl-functionalized glass slide and decanoic ester- and propylamine-linked menthenyl-functionalized surfaces.

Our organic surfaces are characterized using sum frequency generation (SFG),[63−69] a nonlinear vibrational surface spectroscopy technique, and we track the heterogeneous oxidation reactions during exposure to parts per million (ppm) amounts of ozone. Using SFG, the heterogeneous processes are easily monitored with molecular specificity, directly at interfaces, in real time, and with exquisite sensitivity toward molecular orientation. Nonlinear vibrational spectroscopy is also complementary to IR spectroscopy or mass spectrometry based laboratory experiments and yields molecular level information that has already improved our understanding of heterogeneous organic reactions.[70−84] In addition to their relevance to atmospheric chemistry, reactions of organic adlayers on metals and metal oxides are also important in heterogeneous catalysis,[85−87] and we thus extend the pioneering surface spectroscopy experiments of Somorjai,[73−84] Campbell, [88−98] and Nuzzo[99] from metal surfaces toward oxide surfaces, which do not exhibit back-bonding[100] or image dipoles[101] when studied using vibrational spectroscopies.

II. Experimental Section

Our experimental approach for studying organosilane-modified glass and quartz surfaces has been described in the

literature.[70,72,102−111] Briefly, we use a *p*-aniline silane linker, which does not exhibit significant SFG signal in the 2800−3000 cm^{-1} aliphatic CH stretching region and whose aromatic ring is expected to stand up straight with a narrow molecular tilt angle distribution from the surface normal[72] (see Supporting Information). Using acid chloride derivatives of the olefins of interest in this work, we form chemically robust amide bonds to the aniline silane linker. As we will show below, the Kevlar-like properties of our amide-networked aromatic silane linkers prevent their oxidation by ozone, which is a significant advantage over gold−thiol and direct silanization chemistry. A detailed description of the synthetic aspects involved in the preparation of our functionalized surfaces, their characterization by ellipsometry and contact angle measurements, and our laser setup and the spectral analysis are presented in the Supporting Information and previously published work.[72,112]

After spectroscopically analyzing the surface-bound hydrocarbons using SFG and identifying the olefinic CH stretches of interest for the heterogeneous ozonolysis reactions that are important in tropospheric chemistry and catalysis, we place the functionalized substrates into a custom-built Teflon reaction chamber that is held at room temperature and 1 atm of helium and oxygen.[70] The Teflon gas-flow system consists of the appropriate flow meters, Swagelok valves and fittings, a Hg pen ray lamp, a custom-built Teflon chamber, and a custom-built 10 cm path length quartz gas flow cell used for monitoring the ozone absorbance at 254 nm with a UV−vis spectrometer (Ocean Optics, 185−850 nm). The flow setup is shown in Figure 1. After warming the Hg pen ray lamp for approximately 30 min while bypassing the sample chamber, we record the ozone vs time profile along with the SFG spectra. Once the ozone concentration reaches a steady-state level, we direct the ozone flow into the chamber via a three-way valve. At this moment, the time is marked and the reaction time is referenced to 0 s. In general, we expose the surfaces to 1−2 ppm (0.8−1.6 mTorr or (2.6−5.2) × 10^{13} molecules cm^{-3}) of ozone for up to 2 h.

III. Results and Discussion

A. Comparison of Spectral Congestion in Three Different Linker Systems. Figure 2A shows the ssp-polarized SFG spectra obtained from an aniline silane-functionalized glass slide and an aniline silane-linked menthenyl-functionalized glass slide. SFG spectra of propyl amine- and decanoic ester-linked menthenyl-functionalized surfaces, which we discussed in earlier work along with the SFG spectra of the bare linker species,[70] are shown as well. In general, SFG spectra recorded using the ssp polarization combination are sensitive to IR allowed vibrational transitions perpendicular to the surface plane. To account for the fact that the SFG signal intensity of the menthenyl- and the aniline-functionalized surfaces was recorded for 2 and 10 min, respectively, we normalized the SFG spectra to their maximum SFG signal intensity, followed by scaling to comparable signal-to-noise ratios. As mentioned above, the aniline linker does not exhibit significant SFG signal intensity in the 2800−3000 cm^{-1} aliphatic CH stretching region (see Figure 2A and Supporting Information).

To assign the peaks in our SFG spectra, we conducted a systematic analysis by reviewing previously published SFG spectra for similar molecules. We then fit the data with the least number of Lorenztians that will sum together via their phases to generate an accurate fit consistent with literature assignments. For species with no previously published SFG spectra, assignments are made on the basis of surface- and bulk-phase IR and Raman spectra. A detailed explanation of our fitting procedure is found in the Supporting Information.

The SFG spectra of the menthenyl surfaces functionalized with all three linkers show the asymmetric (2950 cm^{-1}) and symmetric (2880 cm^{-1}) CH stretches of CH_3 groups. Through spectral fitting, we assign the modes at 2920 and 2850 cm^{-1} to a CH_2 Fermi resonance and a CH_2 symmetric stretch, respectively.[70] The minor broad signal intensity observed above 3000 cm^{-1} is attributed to the presence of surface-bound water molecules, whose OH stretching region is accessed when the IR laser pulse is tuned toward 3100 cm^{-1}. As discussed in our earlier work,[70] the relative intensities of the ssp-polarized SFG spectra obtained for the propyl amine- and the decanoic ester-linked systems are due to differences in orientation and to spectral overlap from the aliphatic linkers. We conclude from the spectra shown in Figure 2A that the aniline-linked menthenyl system exhibits minimal spectral overlap between the linker and the linked hydrocarbon. This result is further supported by the sps-polarized SFG spectra of the systems under investigation, which are sensitive to vibrational transitions within the surface plane. Figure 2B shows that while overlapping CH stretches are clearly observable for the propylamine- and the decanoic ester-linked systems,[70] the aniline-linked menthenyl systems exclusively displays the asymmetric CH_3 stretch mode at 2960 cm^{-1}. We conclude that the aromatic linker used in our present work is largely spectroscopically silent in the ssp polarization combination. See the Supporting Information for the spectra and further analysis of the aniline silane linker.

B. Unreacted Surfaces: Spectral Assignments. Using the aniline silane linker approach, we prepare glass substrates functionalized with cyclohexene, cyclopentene, and cyclohexane and collect ssp-polarized SFG spectra shown in Figure 3A. All spectra are normalized to the SFG signal intensity at 2850 cm^{-1}. Above 3000 cm^{-1}, the olefinic CH stretches are clearly seen in the ssp-polarized SFG spectra of the cyclohexene- and the cyclopentene-functionalized surfaces, while the cyclohexane spectrum shows only negligible signal contribution in this frequency region.

1. Cyclohexane. Briefly, the ssp-polarized SFG spectrum of the cyclohexane-modified surface displays modes at 2943, 2913, and 2859 cm^{-1}, which we assign via spectral fitting to a CH_2 asymmetric stretch, a CH_2 Fermi resonance, and a CH_2 symmetric stretch, respectively. Within the experimental uncertainty, these assignments agree with valence electron energy loss, high-resolution electron energy loss, SFG, IR, and Raman studies carried out on cyclohexane in the bulk phase or adsorbed at interfaces.[83,98,113−117]

2. Cyclohexene. The ssp-polarized SFG spectrum of the cyclohexene-functionalized glass substrate shows an olefinic CH stretch (3035 cm^{-1}), a CH_2 asymmetric stretch (2924 cm^{-1}), and two CH_2 symmetric stretches (2877 and 2852 cm^{-1}). These assignments agree with IR studies of liquid cyclohexene, cyclohexene monolayers on Au(111), SFG studies of cyclohexene adsorbed to a Pt(111) surface held at 130 K, reflection absorption infrared spectroscopy studies of the cyclohexenyl (C_6H_9) species on Pt(111) held at 250 to 300 K, and high-resolution electron energy loss as well as reflection absorption infrared spectra of cyclohexene bound to Pt(111) held at 95−100 K.[88,99,113,118]

3. Cyclopentene. The ssp-polarized SFG spectrum of the cyclopentene-functionalized glass surfaces shows olefinic stretches at 3060 cm^{-1}, which is in excellent agreement with literature data on neat cyclopentene.[119−122] The position and relative intensities of the symmetric (2880 and 2850 cm^{-1}) and asymmetric (2950 cm^{-1}) CH_2 stretching modes agree with literature infrared and Raman data of neat cyclopentene.[120−122]

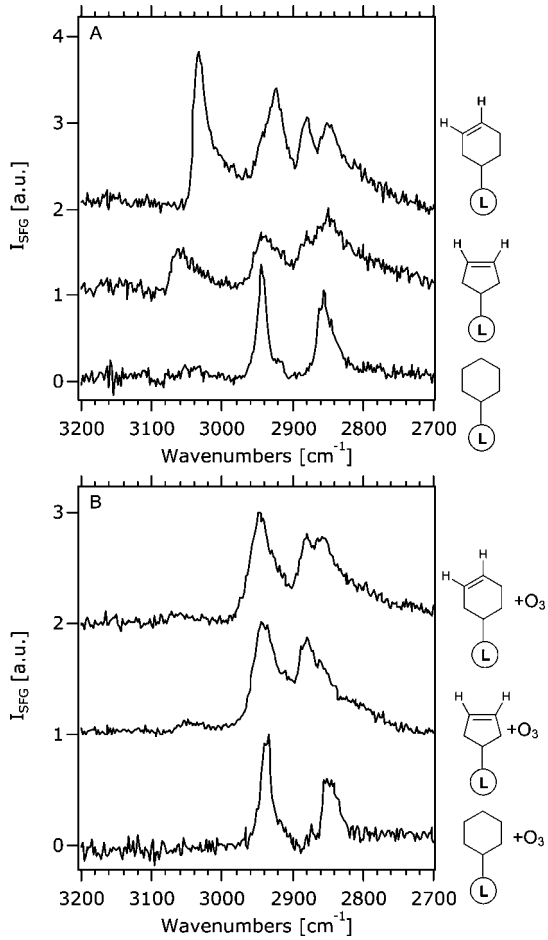

Figure 3. ssp-polarized SFG spectra of aniline-functionalized glass slides linked to (top to bottom) cyclohexene, cyclopentene, and cyclohexane before (A) and after (B) exposure to ozone. Data acquisition times were 2 min. See text for details.

C. Interactions with Ozone. During an ozonolysis reaction, we expect that the interaction of ozone with cyclic olefins would add ozone at the C═C double bond.[3,62,123−125] The reaction begins with a change in the hybridization state on the carbon atoms that form the original C═C double bond as the short-lived primary ozonide is generated (Figure 4). Most proposed reaction pathways in the literature indicate that it then proceeds through an acyclic Criegee intermediate and ends with a variety of oxidation or reduction products, depending on the experimental conditions.[3,62,124,125] A Criegee intermediate is a carbonyl oxide.[126] The two fragments formed by decomposition of the primary ozonide, the Criegee intermediate and an aldehyde, are held in close proximity to one another because they are both surface-bound by the same linker. On the basis of the well-studied gas-phase mechanisms, we expect the intermediate and product species of cyclohexene- and cyclopentene-functionalized glass slides[3,62,124,125] to remain bound to the surface.[127]

1. Surface Products. Figure 3B shows the ssp-polarized SFG spectra recorded after exposing glass slides functionalized with cyclohexene, cyclopentene, and cyclohexane to 1−2 ppm levels of ozone. The cyclohexane system is used as a nonreactive control for the ozonolysis reactions. The SFG spectrum of the cyclohexane-functionalized glass slide after exposure to ozone remains unchanged from the one prior to ozone exposure shown in Figure 3A. This finding strongly suggests that neither the silane linker nor the amide bond linking to the surface species of interest are perturbed in the presence of the low ozone concentrations employed in this work.

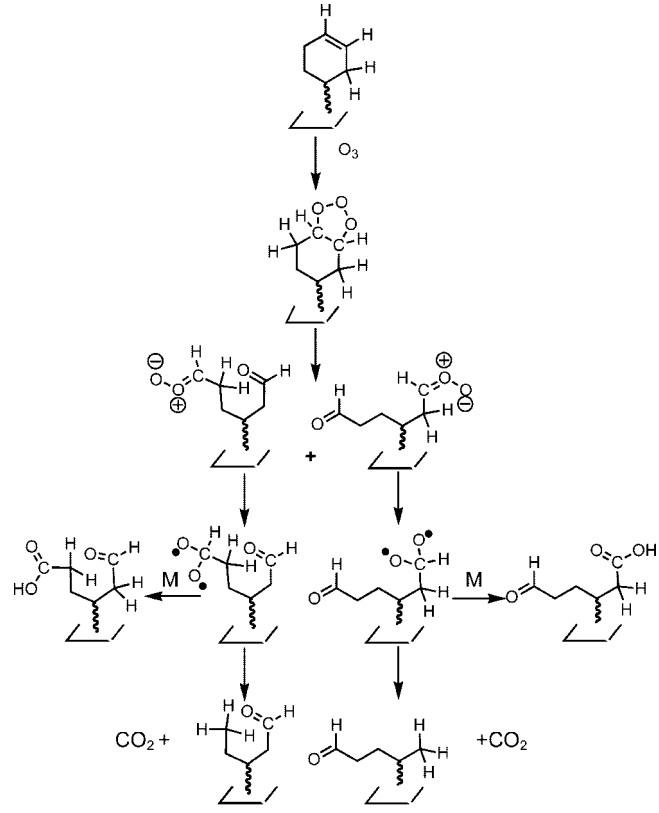

Figure 4. Possible mechanism for the heterogeneous C═C double bond oxidation of cyclohexene by ozone adapted for the surface-bound cyclohexene case from the work of Fenske et al., Thomas et al., and Atkinson and Arey.

2. Cyclohexene and Cyclopentene. In Figure 3B, the disappearance of the olefinic CH stretches in the unsaturated systems (>3000 cm^{-1}) is self-evident. The spectra of cyclohexene before and after exposure to ozone look very different, with the mode at 2924 cm^{-1} decreasing in intensity and a prominent mode at 2945 cm^{-1} emerging. Following exposure to ozone, the ssp-polarized SFG spectra of cyclohexene and cyclopentene exhibit increased SFG signal contributions at 2940−2950 cm^{-1}. Vibrational signatures near 2940−2950 cm^{-1} are typically associated with CH_3 asymmetric stretch modes of aliphatic systems[67,128−133] or with CH stretching modes of unsaturated and saturated cyclic hydrocarbon systems that do not possess methyl groups.[73,134,135]

Previously published experiments involving heterogeneous interactions between ozone and linear alkenes reported the formation of methyl groups. For example, attenuated total reflection infrared spectroscopy studies by Thomas et al. reported the formation of methyl groups and the production of CO_2 when terminal olefin−silanes on glass were exposed to ppm amounts of ozone.[44] Methyl deformation modes at 1460 and 1380 cm^{-1} are also clearly evident in reflection absorption infrared spectra of terminal alkene thiols on gold exposed to an extremely clean and waterless ozone source under ultrahigh-vacuum conditions, which was studied by Fiegland et al.[38] Finally, the diffuse reflection infrared Fourier transform spectra reported by Karagulian et al.,[31] who studied the interaction of ozone with phosphocholines on sodium chloride, also show the presence of modes at 2948 cm^{-1}, which the authors assigned to C−H stretches of the secondary ozonide, but could also be due to methyl group formation. To the best of our knowledge, vibrational assignments of the secondary ozonide CH stretch modes have not been published. However, the formation of

methyl-containing alkanes have been described in reaction pathways by Atkinson and Arey[62] and Finlayson-Pitts and Pitts.[3] Experiments using deuterated olefin C═C double bonds could be used to identify whether CH_3 or CDH_2 species are formed upon ozonolysis. Solid-state NMR experiments by Grassian and co-workers also show the presence of methyl groups in oxidation products.[136] They exposed SiO_2 powder functionalized with c8 alkene silanes to 8 ppb ozone, measured the solid-state ^{13}C NMR before and after ozone exposure, and found a methyl peak in their after-ozone NMR spectrum that was not present in the NMR spectrum recorded prior to ozone exposure.

We observed a marked increase in SFG signal intensity at 2950 cm^{-1} when cyclohexene, cyclopentene, and pentene were exposed to 1−2 ppm ozone levels. In the cyclopentene spectra, a mode of the product species happens to coincide with the 2950 cm^{-1} CH_2 asymmetric stretch observed in the spectrum before ozone exposure. However, the post-ozone-exposure cyclopentene spectrum looks very similar to the spectra after exposure of all the other olefins studied here (cyclohexene and 1-pentene) to ozone.

Our contact angle measurements (vide infra), our SFG surface vibrational spectra, and work published previously by other researchers that we describe above all suggest that the emerging peak at 2950 cm^{-1} may be due to either (1) the formation of methyl groups or (2) the formation of a secondary ozonide. CH stretching modes of saturated cyclic hydrocarbon systems with -CH stretches adjacent to oxygen or nitrogen atoms may shift the CH stretches observed to higher wavenumbers. Here, we address the possibility of methyl formation, which has previously been reported in the literature. Since we do not probe C−O stretches, we assume that secondary ozonide formation may also be occurring.

We note that, in the context of our experimental results regarding the ozonolysis of cyclohexene, cyclopentene, and pentene (vide infra) which all show modes that appear at 2950 cm^{-1}, the increase in intensity at 2950 cm^{-1} for cyclopentene is also consistent with CH_3 formation. With the formation of cyclic structures upon the interaction of ozone with cyclohexene- and cyclopentene-functionalized surfaces being entropically unfavorable, we suggest that the increased SFG signal intensity at 2950 cm^{-1} may be due, at least in part, to the formation of surface-bound methyl groups. Together with the results of Thomas et al.,[44] Fiegland et al.,[38] Karagulian et al.,[31] Usher et al.,[136] Atkinson and Arey,[62] and Finlayson-Pitts and Pitts,[3] the SFG spectra in Figure 3B suggest that the methyl-producing pathway during the ozonolysis of surface-bound C═C double bonds competes with the carboxylic acid- and secondary ozonide-producing pathways and that this scenario is general for surface-bound cyclic and acyclic olefins, be they covalently or electrostatically linked to the surface.

3. Collision Frequency. Figure 4 displays the two pathways that are discussed in this work, which is adapted for the surface-bound cyclohexene case from the work of Fenske et al.,[127] Thomas et al.,[44] and Atkinson and Arey.[62] In general, methyl groups can be formed from vibrationally hot [RCHOO]-like Criegee intermediates that decompose into CO_2 and methyl group containing alkanes. This rearrangement process requires that the Criegee intermediate not be thermalized, which typically occurs in the gas phase via collision partners such as nitrogen. At 1 atm, the collision frequency[137] Z for any species with a collision cross-section similar to that of 2-hexanone (9.85 $Å^2$),[138] which is close to that of the Criegee intermediate generated from cyclohexene, is 1.3×10^{10} s^{-1}, i.e., an average of 80 ps elapses between collisions with atmospheric molecules. For the surface

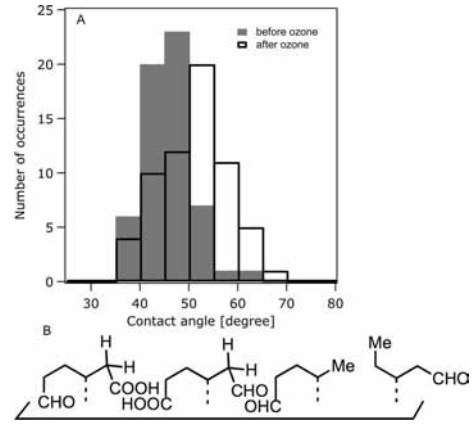

Figure 5. (A) Sessile contact angle distribution with filled gray bars indicating before and empty white bars indicating after ozone exposure. Data set includes 60 measurements each for before and after ozone. For the after ozone measurements, we used slides that had not been previously exposed to water (from contact angle measurements). (B) Plausible ozonolysis products whose hydrophobic and hydrophilic moieties are pointed toward and away from the gas phase, respectively.

case, we scale the surface collision flux, Z_w, to the collision cross-section used above as an upper limit for the area occupied by one surface-bound molecule. This analysis yields a per-molecule surface collision frequency of 2.8×10^9 s^{-1}, which corresponds to an average time between collisions that is about four times longer than what we obtained for the corresponding gas-phase case. Surface-bound Criegee intermediates may therefore remain vibrationally excited for longer time periods than gas-phase Criegee intermediates. Vibrational de-excitation into the covalent linker moieties present in the thiol,[38] silane,[44,70] or charged head groups[31] of the unsaturated systems commonly used for studying heterogeneous organic oxidation chemistry may be of importance as well.

4. Sessile Contact Angle Measurements. To test the notion that the heterogeneous ozonolysis of our olefin surfaces form amphiphilic surface species under our experimental conditions, we carried out contact angle measurements for the cyclohexene-functionalized glass slides before and after ozone exposure (see Supporting Information for details). Our data include 60 measurements each for before and after ozone, which are displayed in the histogram shown in Figure 5A. The sessile contact angles before ozone exposure were 36(6)°, where the number in parentheses indicates the standard deviation in the final digit (1σ). As we discussed in our previous work,[70] these contact angles are low for hydrocarbon systems, which can be attributed to the presence of the highly polar amide group[151] that is part of our linkers. In addition, contact angles on roughened or disorganized hydrocarbons are lower than those for well-ordered alkane systems. Following exposure of the cyclohexene-functionalized glass surface to 1 ppm of ozone, the contact angles were found to increase to 43(6)°. The averages of 36(6) and 43(6)° for the pre- and post-ozone-exposure are not statistically different without further information. Therefore, we use histograms shown in Figure 5A to demonstrate the obvious shift from lower to higher contact angles among all of the 60 measurements made. This increase is in contrast to the 10−20° decrease in contact angles that was observed by Dubowski et al.[139] and also by Thomas et al.,[44] who measured the contact angles of covalently linked linear olefins following ozone exposures that utilized about 10 times higher ozone concentrations when compared to this work. Figure 5B summarizes possible oxidation products, including methyl and

carboxylic acid groups, which are consistent with the mechanism depicted in Figure 4. An important feature of the surface that results from the ozonolysis of a glass slide functionalized with cyclic olefins is that it contains amphiphilic molecules that have long enough molecular flexibility to point their hydrophobic moeities (methyl and methylene groups) toward the nonpolar gas phase and their hydrophilic functional groups (carboxylic acids and aldehydes) toward the polar oxide surface. Intra- and intermolecular hydrogen bonding, which has been reported from nonlinear optics[109] and molecular dynamics simulations[140] to prevent acid ionization in closed space carboxylic acids, is likely to play an important role in the free energy density profile of this heterogeneously oxidized terpene surface because the alternating propionic and acetic acid product species presumably formed here are likely to form molecular dimers that could point away from the gas phase.[141] In general, it thus appears that the ozonolysis of cyclic olefins opens up the hydrocarbon ring to expose the nonpolar center to the nonpolar gas phase, irrespective of what functional groups result from the breaking of the C═C double bond.

D. Time-Dependent Measurements. The olefins we studied exhibit sufficiently high SFG signal intensity in the olefinic and aliphatic CH stretching regions that C═C double bond oxidation reactions can be tracked in real time. By tuning our broadband IR source to a center frequency near 3050 cm^{-1}, we can deliver maximum IR power to the olefinic stretching region and track the olefinic CH stretch, i.e., the surface-bound reactant, and the sp^3 CH stretches of the surface-bound products. We record ssp-polarized SFG spectra every 10 s while exposing cyclohexene-functionalized glass surfaces to around 1 ppm of ozone for 10 min, 30 s, and 10 s. Figures 6 and 7 show the results of these experiments.

Figure 6A is a representative control experiment, in which a cyclohexane-functionalized glass slide was exposed to ~0.5 ppm of ozone. We observe a slight linear increase in the SFG signal at 2945 cm^{-1} that can be attributed to nonreactive hydrophobic interactions of ozone with the saturated hydrocarbon system. This finding is similar to what we reported earlier for octylsilane-functionalized glass surfaces exposed to ozone[70] and is consistent with hydrophobic interactions that have been found to be important in molecular dynamics simulations by Tobias and co-workers, who reported the enrichment of ozone at the terminal methyl groups of aliphatic systems at interfaces.[142] This experiment serves as an important control that shows negligible reactivity in the absence of C═C double bonds and demonstrates that, in the presence of low ozone partial pressures, our silane-based amide-linker system resists ozonation. However, we note that the ozonation of silanes[143] and also hydrocarbons[144] has been reported to occur efficiently, albeit at ozone concentrations that are several orders of magnitude higher than the ones used here.

Parts B−D of Figure 6 show the time-dependent ssp-polarized SFG E-field versus time traces of three cyclohexene-functionalized glass surfaces exposed to about 1 ppm of ozone continuously (Figure 6B) and for 30 s long (Figure 6C) and 10 s long (Figure 6D) pulses. In all time traces, the olefinic CH stretching mode disappears upon exposure of the surface to ozone, and the SFG signal intensity in the aliphatic asymmetric stretching region increases, again immediately upon exposure of the surface to ozone. Under continuous exposure, the reaction is complete after about 3−5 min, which is on a time scale similar to the one reported by Dubowski et al.[41] for terminal olefin silanes, but much quicker than what was reported by Karagulian et al. for pressed pellets of phosphocholines, which contain C═C double bonds near the center of one of the hydrocarbon tails, on powdered salt. Those latter studies show reaction half-lives for the disappearance of the olefinic CH stretches on the order of tens of minutes.[31]

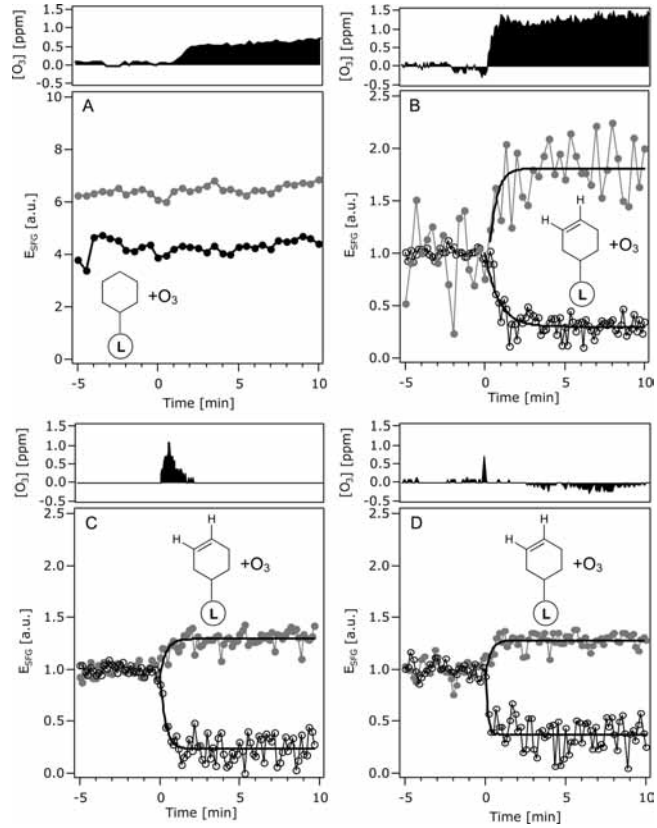

Figure 6. (A) Ozone concentration (top) and SFG E-field of a cyclohexane-functionalized glass slide recorded at 2940 (gray circles) and 2850 cm^{-1} (black circles) as a function of time. (B) Same for a cyclohexene-functionalized glass slide recorded at 2945 (gray circles) and 3030 cm^{-1} (empty circles). (C and D) Same for ozone exposures of 30 and 10 s, respectively. The solid lines are fits to a first-order rate process resulting in the appearance and disappearance of the SFG E-field at 2945 and 3030 cm^{-1}. Please see our previous work for details.

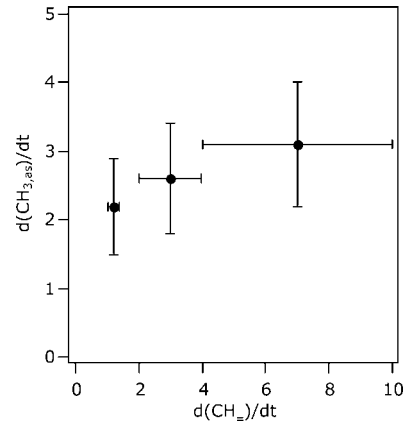

Figure 7. Rates of appearance for the methyl asymmetric CH stretch as a function of disappearance rates for the olefinic CH stretch for the experimental results shown in Figure 4B−D. See text for details.

Assuming that the SFG signal contributions from changes in the molecular re-orientation of the surface-bound species are small, a first-order kinetic fit to the disappearance of the olefinic CH mode at 3030 cm^{-1} results in a rate of 1.2(2) min^{-1}, while the SFG E-field in the aliphatic asymmetric stretching region increases at a rate of 2.2(7) min^{-1}, determined for the 2945

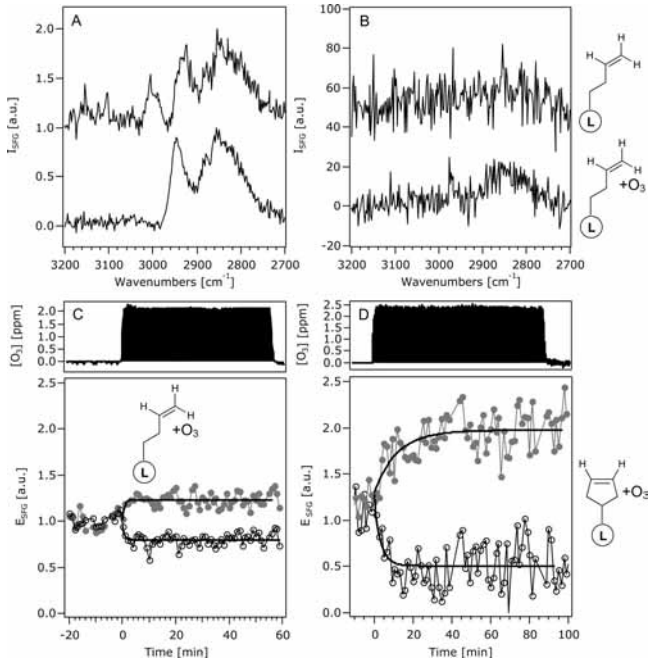

Figure 8. ssp- (A) and sps- (B) Polarized SFG spectrum of an aniline-functionalized glass slide linked to 1-pentene before (top) and after (bottom) exposure to ozone. (C) Ozone concentration (top) and SFG E-field of a 1-pentene-functionalized glass slide recorded at 2945 (gray circles) and 3030 cm^{-1} (black circles) as a function of time. (D) Same for a cyclopentene-functionalized glass slide.

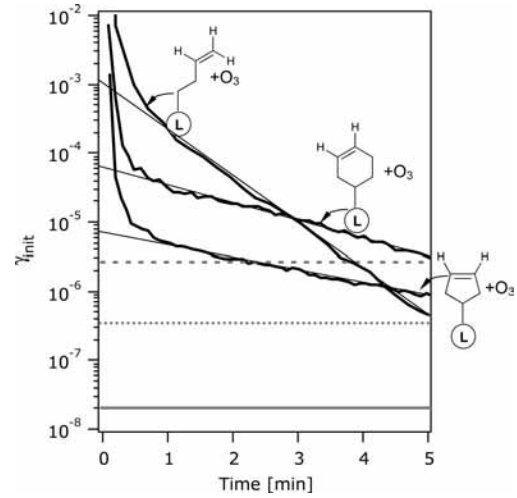

Figure 9. Reactive uptake coefficients, γ, for the first 5 min of exposure to 1−2 ppm of ozone for 1-pentene- (black dotted line), cyclohexene- (black solid line), and cyclopentene-functionalized (black dashed line) glass slides. Horizontal lines correspond to analogous gas-phase reaction probabilities for cyclohexene (gray solid line), 1-pentene (gray dotted line), and cyclopentene (gray dashed line). Thin lines represent the linear extrapolation of the long time responses to short times. Please see text for detail.

cm^{-1} mode. For the disappearance of the olefinic CH mode, the observed rates for the 30 and 10 s long ozone exposures are 3(1) and 7(3) min^{-1}, respectively. For the increase in the aliphatic asymmetric stretch mode, the observed rates are found to be 2.6(8) and 3.1(9) min^{-1} for the 30 and 10 s long ozone exposures, respectively. A weighted fit of the methyl group formation rate dependence on the olefin disappearance rate yields a slope of 0.2(2); that is, the slope ranges from 0 to 0.4. We conclude that the methyl formation rate may increase with the rate at which the olefin reacts away, which is consistent with the notion that the product formation rate is determined by how fast the primary ozonide is formed.

As mentioned by Dubowski et al.,[41] one likely reason for the fact that heterogeneous C═C double bond oxidation reactions are not included in most atmospheric models is the chemical diversity of biogenic and anthropogenic VOCs in the troposphere. After studying the ozonolysis of a cyclohexene-functionalized glass slide in real time, we therefore proceed to search for generalities in the heterogeneous C═C double bond oxidation reactions involving ozone. We begin with a linear olefin, namely, 1-pentene, and continue our work with a surface functionalized with a five-membered cyclic olefin. Figure 8A shows the ssp-polarized SFG spectrum of a 1-pentene-functionalized glass slide before and after exposure to ozone. The olefinic CH stretch mode is observed near 3000 cm^{-1}, and we assign the modes near 2925, 2872, and 2851 cm^{-1} to an asymmetric and two symmetric CH_2 stretches, which agrees well with literature data on liquid 5-chloro-1-pentene and 5-bromo-1-pentene,[145] as well as 1,3-propanediol,[146] ethylene glycol,[147] ethylene diamines,[148] and 1,7-octadiene-functionalized porous silica.[149] After the reaction, we clearly observe SFG signal intensity at 2950 cm^{-1} in the ssp-polarized SFG spectrum, which suggests the formation of surface-bound methyl groups. The weak albeit discernible methyl asymmetric stretch mode at 2985 cm^{-1} in the sps-polarized SFG spectrum (Figure 8B) supports this notion. Figure 8C shows the corresponding kinetic data for an ozone exposure of around 2 ppm, and we find that the olefinic CH stretch mode disappears at a rate of 0.98(42) min^{-1} and that the peak at 2950 cm^{-1} emerges at a rate of 0.5(3) min^{-1}. A representative kinetic run for the ozonolysis of a cyclopentene-functionalized glass slide exposed to around 2 ppm of ozone is shown in Figure 8D. The olefinic CH stretch signal disappears again, and SFG signal intensity at 2950 cm^{-1} increases. We note that both processes occur at rates that are slower (0.3(1) min^{-1} for the olefinic CH stretch and 0.07(2) min^{-1} for the methyl groups) than the rates we obtained for the ozonolysis of the cyclohexene- and the pentene-functionalized glass surfaces. Assuming similar surface coverages, which is reasonable given a comparable molecular footprint of cyclohexene and cyclopentene, we conclude that the five-membered cyclic olefin reacts about 10 times slower than the six-membered cyclic olefin. The apparent discrepancy with gas-phase data, which show the opposite,[62] will be discussed below.

E. Initial Reactive Uptake Coefficients. Reactive uptake coefficients[41] are commonly used in atmospheric chemistry models to quantify how many heterogeneous reactions result from the collisions of reactive gas-phase species with an aerosol particle surface. Explicit heterogeneous rate expressions for the heterogeneous C═C double bond oxidation by ozone, which typically contain the ozone concentration in the gas phase,[70] are available as well. Following Dubowski et al.[41] and also described in our previous work,[70] we determined the initial reactive uptake coefficients (described in detail in the Supporting Information) for the interactions of the cyclohexene-, the cyclopentene-, and the 1-pentene-modified glass surfaces with 1.75 ppm ozone under steady-state conditions. The result is shown in Figure 9 for the first 5 min of the interaction. The reactive uptake coefficient for cyclohexene is found to range between 10^{-2} and 10^{-4} in the first 30 s. The remainder of the interaction which occurs between 0 and 5 min is characterized by a decay in which γ approaches 10^{-6} as surface reaction sites are depleted. Extrapolating this decay to zero time yields an intercept of $6(1) \times 10^{-5}$, which we report as the initial reactive uptake coefficient for 1.75 ppm of ozone interacting with

cyclohexene-functionalized glass surfaces. Interestingly, this initial reactive uptake coefficient for cyclohexene is about 200 times higher than the gas phase reaction probability (3.5×10^{-7}), which is calculated[62,70] for the ozonolysis of cyclohexene using basic collision theory and kinetic rate data compiled by Atkinson and Arey ($k_{rxn} = 8.1 \times 10^{-17}$ cm^3 molecule^{-1} s^{-1} at 298 K).[62] This enhancement in the surface vs gas-phase reactivity is comparable to the one we reported earlier for the interaction of ozone with menthenyl-functionalized glass surfaces.[70] Our γ values are similar to those obtained by Usher et al. through solid-state NMR ozone experiments (10^{-4}).[136]

Figure 9 also shows the initial reactive uptake coefficient that we obtained for our 1-pentene-functionalized surfaces. The initial reactive uptake coefficient for 2 ppm of ozone is found to be 1×10^{-3}, which is more than 1 order of magnitude above that of cyclohexene, and around 2−3 orders of magnitude above the initial reactive uptake coefficient reported by Dubowski et al. for c3- and c8-functionalized surfaces at the same ozone partial pressure.[41] Furthermore, the enhancement of the heterogeneous process measured on our surfaces over the gas phase reaction probability of 1-pentene (2×10^{-8}) is substantial. Finally, the initial reactive uptake coefficient for our cyclopentene-functionalized surfaces is found to be 1×10^{-5}, which is about four to five times higher than the corresponding gas phase reaction probability (2.5×10^{-6}).

A comparison of the reactive uptake coefficients for cyclohexene and the menthenyl cases suggests that the well-known rate-enhancing electronic effect of the methyl group in the menthenyl moiety is outpaced by the increased C═C double bond accessibility of surface-bound cyclohexene, which does not contain a sterically hindering methyl group. Similarly, the π-electron system of our 1-pentene-functionalized surfaces is likely to be more accessible than that of the terminal c3 and c8 alkene silanes studied by Dubowski et al.,[41] who reported calculated distributions of orientation angles made by the C═C double bonds that peak near 0° from the surface normal. This orientation is orthogonal to the optimal angle of approach that would yield an efficient reaction and is shifted by 45° from the C═C double bond angle expected for our amide-bonded 1-pentene system, thus reconciling the difference in γ values.

We note that the gas phase reactivity data on the ozonolysis of 1-pentene and cyclohexene shows that the latter should react about eight times faster than the former.[62] However, while all of our aniline-linked olefins can rotate about the carbon−carbon bond adjacent to the amide carbonyl group, additional rotations around carbon−carbon bonds are not possible in the cyclic structures, whereas rotations around two additional carbon−carbon bonds are possible in the case of the linear pentene system. Thus, our data suggest that the higher initial reactive uptake coefficient of the linear vs the cyclic olefins is due to the increased floppiness of the linear olefin, which increases the access of the C═C double bond to ozone. Given the fact that the system under investigation is unlikely to be catalytic at the level of a system catalyzed by metal surfaces, we can assume that the reaction probability between one ozone molecule and one C═C double bond at the surface should be equal to that of the gas-phase case unless unreactive collisions of ozone with the surface-bound organic species significantly reduces its kinetic energy. To obtain an upper limit of the number of attempts that each ozone molecule will make to react with one C═C double bond, we take the initial reaction probabilities determined from our surface measurements and divide them by the gas phase reaction rate. For cyclohexene, this number is found to be around 2×10^2, and for 1-pentene, it is found to be around 5×10^4, which is again consistent with an increased floppiness of the linear olefin. We note that this situation would be quite different in long-range two-dimensional crystalline organic adlayers of straight-chain hydrocarbons, i.e., self-assembled monolayers (SAMs), which are known to contain a negligible number density of gauche defects and to be well-packed. There are no reports available in the literature showing formation of long-range, two-dimensional crystalline or semicrystalline organic adlayers, i.e., SAMs,[150] when glass slides are functionalized with organosilanes. This suggests that our argument regarding 1-pentene floppiness and the resulting increase in C═C double bond accessibility should hold for the systems under investigation in this work.

Finally, the data displayed in Figure 6D clearly show that short ozone exposures on the order of 10 s can kick-start the heterogeneous ozonolysis, after which the reactions continue even when the gas-phase ozone concentration is below the detection limit. Time-limited ozone exposure conditions could include scenarios in which aerosol particles pass through ozone-rich air, when aerosols pass across polluted areas and into remote regions with low background ozone concentrations, or when aerosol particles are mixed with ozone-rich air in eddies, such as those commonly encountered in polluted urban areas. In these cases, we would expect the heterogeneous chemistry to occur long after the aerosols passed through air that contained high ozone concentrations, and modifications to existing γ expressions may be required to account for this effect. The continuing chemistry shown in Figure 6D could be due to small amounts of ozone present in the sample chamber after the ozone pulse which are below detection levels. In addition, while the ozone concentrations used in this work are low when compared to many experimental laboratory studies available in the literature, they are still a factor of 5−10 higher than the maximum allowable short-period concentration of ozone. Thus, even our 10 s exposure time may be long enough at the concentrations employed in this work to react with the entire surface film.[2]

IV. Summary

In conclusion, we have studied the heterogeneous reactions of ozone with cyclic alkenes covalently linked to oxide surfaces which serve as models for studying the oxidation of biogenic terpenes adsorbed to mineral aerosol surfaces. We measured polarization-resolved vibrational sum frequency generation spectra of glass surfaces functionalized with 1-pentene, 2-hexene, cyclopentene, cyclohexene, and a menthenol derivative. Vibrational sum frequency generation was also used to track the C═C double bond oxidation reactions initiated by ozone in real time and to characterize the surface-bound product species, which exhibit vibrational signatures consistent with methyl groups, but do not rule out the formation of other products. Together with contact angle measurements, our result suggests that reaction pathways involving vibrationally hot Criegee intermediates strongly compete with pathways that involve thermalized surface species. Kinetic measurements suggest that the rate-limiting step in the heterogeneous C═C double bond oxidation reactions is likely to be the formation of the primary ozonide. From the determination of the reactive uptake coefficients, we found that ozone molecules undergo between 100 and 10000 unsuccessful collisions with C═C double bonds before the reaction occurs. The magnitudes of the reactive uptake coefficients for the cyclic and linear olefins studied here do

not follow the corresponding gas-phase reactivities but are rather correlated with the accessibility of the C=C double bonds at the surface. Future work will further increase the complexity of the organic adlayers and address the role of chirality in heterogeneous organic oxidation reactions of terpenes.

Acknowledgment. G.Y.S. gratefully acknowledges support by NASA Headquarters under the NASA Earth and Space Science Fellowship program (Grant 07-Earth07R-0084). J.M.G.-D. gratefully acknowledges a fellowship from the Camille and Henry Dreyfus Postdoctoral Program in Environmental Chemistry. We gratefully acknowledge Neil Donahue for helpful discussions. Support for this project is provided by the National Science Foundation Atmospheric Chemistry division (Grant NSF-ATM 0533634), the ACS Petroleum Research Fund, the Director, Chemical Sciences, Geosciences and Biosciences Division, of the U.S. Department of Energy (Grant DE-FG02-06ER15787), and a National Science Foundation CAREER grant in Experimental Physical Chemistry (Grant NSF CHEM EPC 0348873). Support from the DOE-funded Northwestern University Institute for Catalysis in Energy Processes (ICEP) (Grant DE-FG02-03-ER15457/A004) and the Northwestern University International Institute for Nanotechnology (IIN) is greatly appreciated. F.M.G. is a Sloan Foundation Fellow. The authors also acknowledge donations, equipment loans, and the technical support of Spectra Physics, a Division of Newport Corp.

Supporting Information Available: Text describing additional experimental procedures, calculations of the orientation of the methyl group of *p*-tolyl-silane functionalized glass slides, rate constants, and gamma values. Figures are included which show 1) the ssp-polarized spectrum of a glass slide functionalized with an aniline silane and 2) the sps-polarized spectrum of a 1-pentene-functionalized glass slide after ozone exposure before summation using the hybride scanning-tuning method. This material is available free of charge via the Internet at http://pubs.acs.org.

References and Notes

(1) IPCC, 2007: Summary for Policymakers. In *Climate Change 2007: The Physical Science Basis. Contribution of Working Group I to the Fourth Assessment Report of the Intergovernmental Panel on Climate Change*; Cambridge University Press: Cambridge, U.K., 2007.

(2) Seinfeld, J. H.; Pandis, S. N. *Atmos. Chem. Phys.*; John Wiley & Sons: New York, 1998.

(3) Finlayson-Pitts, B. J., Jr. *Chemistry of the Upper and Lower Atmosphere*; Academic Press: New York, 2000.

(4) Ravishankara, A. R. *Science* **1997**, *276*, 1058.

(5) Underwood, G. M.; Song, C. H.; Phadnis, M.; Carmichael, G. R.; Grassian, V. H. *J. Geophys. Res., [Atmos.]* **2001**, *106*, 18055.

(6) Zhang, Y.; Carmichael, G. R. *J. Appl. Meteorol.* **1999**, *38*, 353.

(7) Raes, F.; Bates, T.; McGovern, F.; Van Liedekerke, M. *Tellus, Ser. B* **2000**, *52*, 111.

(8) de Reus, M.; Strom, J.; Curtius, J.; Pirjola, L.; Vignati, E.; Arnold, F.; Hansson, H. C.; Kulmala, M.; Lelieveld, J.; Raes, F. *J. Geophys. Res., [Atmos.]* **2000**, *105*, 24751.

(9) de Reus, M.; Dentener, F.; Thomas, A.; Borrmann, S.; Strom, J.; Lelieveld, J. *J. Geophys. Res., [Atmos.]* **2000**, *105*, 15263.

(10) Visible Earth: A Catalog of Images and Animations of Our Home Planet, Halusa, Guran. http://visibleearth.nasa.gov/view_set.php?categoryID=117. Accessed October 13, 2008.

(11) Parrington, J. R. *Science* **1983**, *220*, 666.

(12) Parrington, J. R.; Zoller, W. H.; Aras, N. K. *Science* **1983**, *220*, 195.

(13) Neff, J. C.; Ballantyne, A. P.; Farmer, G. L.; Mahowald, N. M.; Conroy, J. L.; Landry, C. C.; Overpeck, J. T.; Painter, T. H.; Lawrence, C. R.; Reynolds, R. L. *Nat. Geosci.*, **2008**, *1*, 189–195.

(14) Prospero, J. M.; Barrett, K.; Church, T.; Dentener, F.; Duce, R. A.; Galloway, J. N.; Levy, H.; Moody, J.; Quinn, P. *Biogeochemistry* **1996**, *35*, 27.

(15) NASA Code 916, Atmospheric Chemistry and Dynamics Branch, 1998.

(16) Pimentel, D.; Harvey, C.; Resosudarmo, P.; Sinclair, K.; Kurz, D.; McNair, M.; Crist, S.; Shpritz, L.; Fitton, L.; Saffouri, R.; Blair, R. *Science* **1995**, *269*, 464.

(17) Pimentel, D.; Harvey, C.; Resosudarmo, P.; Sinclair, K.; Kurz, D.; McNair, M.; Crist, S.; Shpritz, L.; Fitton, L.; Saffouri, R.; Blair, R. *Science* **1995**, *267*, 1117.

(18) Trimble, S. W.; Crosson, P. *Science* **2000**, *290*, 1301.

(19) Trimble, S. W.; Crosson, P. *Science* **2000**, *289*, 248.

(20) Wienhold, B. J.; Luchiari, A.; Zhang, R. *Ann. Arid Zone* **2000**, *39*, 333.

(21) Wienhold, B. J.; Power, J. F.; Doran, J. W. *Soil Sci.* **2000**, *165*, 13.

(22) Nieuwenhuijsen, M. J.; Schenker, M. B. *Am. Ind. Hyg. Assoc. J.* **1998**, *59*, 9.

(23) Schenker, M. *Environ. Health Perspect.* **2000**, *108*, 661.

(24) Schenker, M. B.; Orenstein, M. R.; Saiki, C. L.; Samuels, S. J. *Am. J. Respir. Crit. Care Med.* **1999**, *159*, A297.

(25) Zuberi, B.; Bertram, A. K.; Koop, T.; Molina, L. T.; Molina, M. J. *J. Phys. Chem. A* **2001**, *105*, 6458.

(26) Baker, M. *Nature* **2001**, *413*, 586.

(27) Martin, S. T. *Chem. Rev.* **2000**, *100*, 3403.

(28) Prupacher, H. R.; Klett, J. D. *Microphysics of Clouds and Precipitation*; Kluwer Academic Press: Boston, MA, 1997.

(29) Murphy, D. M.; Thomson, D. S.; Mahoney, M. J. *Science* **1998**, *282*, 1664.

(30) Rogge, W. F.; Hildemann, L. M.; Mazurek, M. A.; Cass, G. R.; Simoneit, B. R. T. *Environ. Sci. Technol.* **1991**, *25*, 1112.

(31) Karagulian, F.; Lea, A. S.; Dilbeck, C. W.; Finlayson-Pitts, B. J. *Phys. Chem. Chem. Phys.* **2008**, *10*, 528.

(32) Rudich, Y. *Chem. Rev.* **2003**, *103*, 5097.

(33) Gill, P. S.; Graedel, R. E.; Weschler, C. J. *Rev. Geophys.* **1983**, *21*, 903.

(34) Ellison, G. B.; Tuck, A. F.; Vaida, V. *J. Geophys. Res.* **1999**, *104*, 11633.

(35) Eliason, T. L.; Gilman, J. B.; Vaida, V. *Atmos. Environ.* **2004**, *38*, 1367.

(36) Eliason, T. L.; Aloisio, S.; Donaldson, D. J.; Cziczo, D. J.; Vaida, V. *Atmos. Environ.* **2003**, *37*, 2207.

(37) Northway, M. J.; de Gouw, J. A.; Fahey, D. W.; Gao, R. S.; Warneke, C.; Roberts, J. M.; Flocke, F. *Atmos. Environ.* **2004**, *38*, 6017.

(38) Fiegland, L. R.; McCorn Saint Fleur, M.; Morris, J. R. *Langmuir* **2005**, *21*, 2660.

(39) Lai, C. C.; Yang, S. H.; Finlayson-Pitts, B. J. *Langmuir* **1994**, *10*, 4637.

(40) Wadia, Y.; Tobias, D. J.; Stafford, R.; Finlayson-Pitts, B. J. *Langmuir* **2000**, *16*, 9321.

(41) Dubowski, Y.; Vieceli, J.; Tobias, D. J.; Gomez, A.; Lin, A.; Nizkorodov, S. A.; McIntire, T. M.; Finlayson-Pitts, B. J. *J. Phys. Chem. A* **2004**, *108*, 10473.

(42) Usher, C. R.; Michel, A. E.; Grassian, V. H. *Chem. Rev.* **2003**, *103*, 4883.

(43) Moise, T.; Rudich, Y. *J. Geophys. Res., [Atmos.]* **2000**, *105*, 14667.

(44) Thomas, E. R.; Frost, G. J.; Rudich, Y. *J. Geophys. Res., [Atmos.]* **2001**, *106*, 3045.

(45) Poschl, U.; Letzel, T.; Schauer, C.; Niessner, R. *J. Phys. Chem. A* **2001**, *105*, 4029.

(46) Mmereki, B. T.; Donaldson, D. J. *J. Phys. Chem. A* **2003**, *107*, 11038.

(47) Moise, T.; Rudich, Y. *J. Phys. Chem. A* **2002**, *106*, 6469.

(48) Katrib, Y.; Martin, S. T.; Hung, H. M.; Rudich, Y.; Zhang, H. Z.; Slowik, J. G.; Davidovits, P.; Jayne, J. T.; Worsnop, D. R. *J. Phys. Chem. A* **2004**, *108*, 6686.

(49) Smith, G. D.; Woods, E.; DeForest, C. L.; Baer, T.; Miller, R. E. *J. Phys. Chem. A* **2002**, *106*, 8085.

(50) Thornberry, T.; Abbatt, J. P. D. *Phys. Chem. Chem. Phys.* **2004**, *6*, 84.

(51) Hearn, J. D.; Lovett, A. J.; Smith, G. D. *Phys. Chem. Chem. Phys.* **2005**, *7*, 501.

(52) Hearn, J. D.; Smith, G. D. *J. Phys. Chem. A* **2004**, *108*, 10019.

(53) Morris, J. W.; Davidovits, P.; Jayne, J. T.; Jimenez, J. L.; Shi, Q.; Kolb, C. E.; Worsnop, D. R.; Barney, W. S.; Cass, G. *Geophys. Res. Lett.* **2002**, 29.

(54) Jang, M. S.; Carroll, B.; Chandramouli, B.; Kamens, R. M. *Environ. Sci. Technol.* **2003**, *37*, 3828.

(55) Morris, J. W.; Davidovits, P.; Jayne, J. T.; Jimenez, J. L.; Shi, Q.; Kolb, C. E.; Worsnop, D. R.; Barney, W. S.; Cass, G. *Geophys. Res. Lett.* **2002**, *29*, 71/1.

(56) Voss, L. F.; Hadad, C. M.; Allen, H. C. *J. Phys. Chem. B* **2006**, *110*, 19487.
(57) McIntire, T. M.; Lea, S. A.; Gaspar, D. J.; Jaitly, N.; Dubowski, Y.; Li, Q.; Finlayson-Pitts, B. J. *Phys. Chem. Chem. Phys.* **2006**, *7*, 3605.
(58) Hearn, J. D.; Smith, G. D. *J. Phys. Chem. A* **2007**, *111*, 11059.
(59) McNeill, V. F.; Wolfe, G. M.; Thornton, J. A. *J. Phys. Chem. A* **2007**, *111*, 1073.
(60) Knopf, D. A.; Anthony, L. M.; Bertram, A. K. *J. Phys. Chem. A* **2005**, *109*, 5579.
(61) Grassian, V. H. *J. Phys. Chem. A* **2002**, *106*, 860.
(62) Atkinson, R.; Arey, J. *Chem. Rev.* **2003**, *103*, 4605.
(63) Zhu, X. D.; Suhr, H. J.; Shen, Y. R. *J. Opt. Soc. Am. B* **1986**, *3*, P252.
(64) Shen, Y. R. *The Principles of Nonlinear Optics*; John Wiley & Sons: New York, 1984.
(65) Eisenthal, K. B. Equilibrium and Dynamic Processes at Interfaces by Second Harmonic and Sum Frequency Generation. In *Annual Review of Physical Chemistry*; Strauss, H. L., Babcock, G. T., Leone, S. R., Eds.; Annual Reviews: Palo Alto, CA, 1992; Vol. 43; p 627.
(66) Gopalakrishnan, S.; Liu, D.; Allen, H. C.; Kuo, M.; Shultz, M. J. *Chem. Rev.* **2006**, *106*, 1155.
(67) Richter, L. J.; Petralli-Mallow, T. P.; Stephenson, J. C. *Opt. Lett.* **1998**, *23*, 1594.
(68) Eliel, E. R.; van der Ham, E. W. M.; Vrehen, Q. H. F.; Barmentlo, M.; t Hooft, G. W.; van der Meer, A. F. G.; van Amersfoort, P. W. *Nucl. Instrum. Methods A* **1994**, *341*, 152.
(69) Schaller, R. D.; Johnson, J. C.; Wilson, K. R.; Lee, L. F.; Haber, L. H.; Saykally, R. J. *J. Phys. Chem. B* **2002**, *106*, 5143.
(70) Voges, A. B.; Stokes, G. Y.; Gibbs-Davis, J. M.; Lettan, R. B.; Bertin, P. A.; Pike, R. C.; Nguyen, S. T.; Scheidt, K. A.; Geiger, F. M. *J. Phys. Chem. C* **2007**, *111*, 1567.
(71) Voss, L. F.; Bazerbashi, M. F.; Beekman, C. P.; Hadad, C. M.; Allen, H. C. *J. Geophys. Res.* **2007**, *112*, D06209.
(72) Stokes, G. Y.; Buchbinder, A. M.; Gibbs-Davis, J. M.; Scheidt, K. A.; Geiger, F. M. Invited Article for Vibrational Spectroscopy, in press.
(73) Yang, M. C.; Chou, K. C.; Somorjai, G. A. *J. Phys. Chem. B* **2004**, *108*, 14766.
(74) Cremer, P. S.; Su, X. C.; Shen, Y. R.; Somorjai, G. *J. Chem. Soc., Faraday Trans.* **1996**, *92*, 4717.
(75) Cremer, P. S.; Su, X. C.; Shen, Y. R.; Somorjai, G. A. *J. Phys. Chem.* **1996**, *100*, 16302.
(76) Su, X. C.; Jensen, J.; Yang, M. X.; Salmeron, M. B.; Shen, Y. R.; Somorjai, G. A. *Faraday Discuss.* **1996**, 263.
(77) Su, X. C.; Cremer, P. S.; Shen, Y. R.; Somorjai, G. A. *Phys. Rev. Lett.* **1996**, *77*, 3858.
(78) Cremer, P. S.; Su, X. C.; Shen, Y. R.; Somorjai, G. A. *J. Am. Chem. Soc.* **1996**, *118*, 2942.
(79) Su, X. C.; Shen, Y. R.; Somorjai, G. A. *Chem. Phys. Lett.* **1997**, *280*, 302.
(80) Cremer, P. S.; Su, X. C.; Shen, Y. R.; Somorjai, G. A. *J. Phys. Chem. B* **1997**, *101*, 6474.
(81) Su, X. C.; Cremer, P. S.; Shen, Y. R.; Somorjai, G. A. *J. Am. Chem. Soc.* **1997**, *119*, 3994.
(82) Yang, M.; Somorjai, G. A. *J. Phys. Chem. B* **2004**, *108*, 4405.
(83) Yang, M.; Somorjai, G. A. *J. Am. Chem. Soc.* **2003**, *125*, 11131.
(84) Yang, M.; Chou, K. C.; Somorjai, G. A. *J. Phys. Chem. B* **2003**, *107*, 5267.
(85) Ma, Z.; Zaera, F. *Surf. Sci. Rep.* **2006**, *61*, 229.
(86) De Vos, D. E.; Dams, M.; Sels, B. F.; Jacobs, P. A. *Chem. Rev.* **2002**, *102*, 3615.
(87) Buriak, J. M. *Chem. Rev.* **2002**, *102*, 1271.
(88) Henn, F. C.; Diaz, A. L.; Bussell, M. E.; Hugenschmidt, M. B.; Domagala, M. E.; Campbell, C. T. *J. Phys. Chem.* **1992**, *96*, 5965.
(89) Domagala, M. E.; Campbell, C. T. *J. Vacuum Sci. Technol., A* **1993**, *11*, 2128.
(90) Domagala, M. E.; Campbell, C. T. *Langmuir* **1994**, *10*, 2636.
(91) Domagala, M. E.; Campbell, C. T. *Surf. Sci.* **1994**, *301*, 151.
(92) Xu, C.; Koel, B. E.; Newton, M. A.; Frei, N. A.; Campbell, C. T. *J. Phys. Chem.* **1995**, *99*, 16670.
(93) Frei, N. A.; Campbell, C. T. *J. Phys. Chem.* **1996**, *100*, 8402.
(94) Campbell, C. T. *J. Chem. Soc., Faraday Trans.* **1996**, *92*, 1435.
(95) Newton, M. A.; Campbell, C. T. *Catal. Lett.* **1996**, *37*, 15.
(96) Newton, M. A.; Campbell, C. T. *Z. Phys. Chem. (Muenchen)* **1997**, *198*, 169.
(97) Hugenschmidt, M. B.; Diaz, A. L.; Campbell, C. T. *J. Phys. Chem.* **1992**, *96*, 5974.
(98) Bussell, M. E.; Henn, F. C.; Campbell, C. T. *J. Phys. Chem.* **1992**, *96*, 5978.
(99) Manner, W. L.; Girolami, G. S.; Nuzzo, R. G. *J. Phys. Chem. B* **1998**, *102*, 10295.
(100) Höfer, U. *Appl. Phys. A: Mater. Sci. Process.* **1996**, *63*, 533.
(101) Roeterdink, W. G.; Berg, O.; Bonn, M. *J. Chem. Phys.* **2004**, *121*, 10174.
(102) Hayes, P. L.; Gibbs-Davis, J. M.; Musorrafiti, M. J.; Mifflin, A. L.; Scheidt, K. A.; Geiger, F. M. *J. Phys. Chem. C* **2007**, *111*, 8796.
(103) Gibbs-Davis, J. M.; Hayes, P. L.; Scheidt, K.; Geiger, F. M. *J. Am. Chem. Soc.* **2007**, *129*, 7175.
(104) Stokes, G. Y.; Boman, F. C.; Gibbs-Davis, J. M.; Stepp, B. R.; Condie, A.; Nguyen, S. T.; Geiger, F. M. *J. Am. Chem. Soc.* **2007**, *129*, 7492.
(105) Mifflin, A. L.; Konek, C. T.; Geiger, F. M. *J. Phys. Chem. B* **2006**, *110*, 22577.
(106) Al-Abadleh, H. A.; Mifflin, A. L.; Bertin, P. A.; Nguyen, S. T.; Geiger, F. M. *J. Phys. Chem. B* **2005**, *109*, 9691.
(107) Al-Abadleh, H. A.; Mifflin, A. L.; Musorrafiti, M. J.; Geiger, F. M. *J. Phys. Chem. B* **2005**, *109*, 16852.
(108) Al-Abadleh, H. A.; Voges, A. B.; Bertin, P. A.; Nguyen, S. T.; Geiger, F. M. *J. Am. Chem. Soc.* **2004**, *126*, 11126.
(109) Konek, C. T.; Musorrafiti, M. J.; Al-Abadleh, H. A.; Bertin, P. A.; Nguyen, S. T.; Geiger, F. M. *J. Am. Chem. Soc.* **2004**, *126*, 11754.
(110) Voges, A. B.; Al-Abadleh, H. A.; Geiger, F. M. Applications of Nonlinear Optical Techniques for Studying Heterogeneous Systems Relevant in the Natural Environment. In *Environmental Catalysis*; Grassian, V. H. , Ed., CRC Publishing: Boca Raton, FL, 2005; p 83.
(111) Voges, A. B.; Al-Abadleh, H. A.; Musorrafiti, M. J.; Bertin, P. A.; Nguyen, S. T.; Geiger, F. M. *J. Phys. Chem. B.* **2004**, *108*, 18675.
(112) Zhang, F.; Srinivasan, M. P. *Langmuir* **2004**, *20*, 2309.
(113) Syomin, D.; Koel, B. E. *Surf. Sci.* **2002**, *498*, 61.
(114) Sheppard, N. *Annu. Rev. Phys. Chem.* **1988**, *39*, 589.
(115) Sheppard, N.; De la Cruz, C. *Adv. Catal.* **1998**, *42*, 181.
(116) Obremski, R. J.; Brown, C. W.; Lippinco, E. R. *J. Chem. Phys.* **1968**, *49*, 185.
(117) Takahashi, H.; Shimanouchi, T. *J. Mol. Spectrosc.* **1964**, *13*, 43.
(118) Somorjai, G. A.; Rupprechter, G. *J. Phys. Chem. B* **1999**, *103*, 1623.
(119) Villarreal, J. R.; Laane, J.; Bush, S. F.; Harris, W. C. *Spectrochim. Acta* **1979**, *35A*, 331.
(120) Beckett, C. W.; Pitzer, K. S. *J. Am. Chem. Soc.* **1948**, *70*, 4227.
(121) Allen, W. D.; Csaszar, A. G.; Horner, D. A. *J. Am. Chem. Soc.* **1992**, *114*, 6834.
(122) Lespade, L.; Cavagnat, D.; Rodin-Bercion, S. *J. Phys. Chem. A* **2000**, *104*, 9880.
(123) Bailey, P. S. *Ozonation in Organic Chemistry*; Academic Press: New York, 1978.
(124) Vollhardt, K. P. C.; Schore, N. E. *Organic Chemistry: Structure and Function*, 3rd ed.; W. H. Freeman: New York, 1999.
(125) March, J. *Advanced Organic Chemistry: Reactions, Mechanisms, and Structure*, 4th ed.; Wiley & Sons: New York, 1992.
(126) Criegee, R. *Angew. Chem., Int. Ed. Engl.* **1975**, *14*, 745.
(127) Fenske, J. D.; Kuwata, K. T.; Houk, K. N.; Paulson, S. E. *J. Phys. Chem. A* **2000**, *104*, 7246.
(128) Shen, Y. R. *Nature* **1989**, *337*, 519.
(129) Liu, Y.; Wolf, L. K.; Messmer, M. C. *Langmuir* **2001**, *17*, 4329.
(130) Chen, C. Y.; Loch, C. L.; Wang, J.; Chen, Z. *J. Phys. Chem. B* **2003**, *107*, 10440.
(131) Esenturk, O.; Walker, R. A. *J. Phys. Chem. B* **2004**, *108*, 10631.
(132) Eisenthal, K. B. *Chem. Rev.* **1996**, *96*, 1343.
(133) Himmelhaus, N.; Eisert, F.; Buck, M.; Grunze, M. *J. Phys. Chem. B* **2000**, *104*, 576.
(134) Boatz, J. A.; Gordon, M. S.; Hilderbrandt, R. L. *J. Am. Chem. Soc.* **1988**, *110*, 352.
(135) Su, X. C.; Kung, K. Y.; Lahtinen, J.; Shen, Y. R.; Somorjai, G. A. *J. Mol. Catal. A: Chem.* **1999**, *141*, 9.
(136) Usher, C. R.; Michel, A. E.; Stec, D.; Grassian, V. H. *Atmos. Environ.* **2003**, *37*, 5337.
(137) Atkins, P.; de Paula, J. *Physical Chemistry*, 7th ed.; W. H. Freeman: New York, 2002.
(138) van Houte, J. J.; de Koster, C. G.; van Thuiji, J. *Int. J. Mass Spectrom. Ion Process.* **1992**, *115*, 173.
(139) Dubowski, Y.; Vieceli, J.; Tobias, D. J.; Gomez, A.; Lin, A.; Nizkorodov, S. A.; McIntire, T. M.; Finlayson-Pitts, B. J. *J. Phys. Chem. A* **2004**, *108*, 10473.
(140) Winter, N.; Vieceli, J.; Benjamin, I. *J. Phys. Chem. B* **2008**, *112*, 227.
(141) Grimm, R. L.; Barrentine, N. M.; Knox, C. J. H.; Hemminger, J. C. *J. Phys. Chem. C* **2008**, *112*, 890.
(142) Vieceli, J.; Ma, O. L.; Tobias, D. J. *J. Phys. Chem. A* **2004**, *108*, 5806.
(143) Cerkovnik, J.; Tuttle, T.; Kraka, E.; Lendero, N.; Plesnicar, B.; Cremer, D. *J. Am. Chem. Soc.* **2006**, *128*, 4090.
(144) Olah, G. A.; Yoneda, N.; Parker, D. G. *J. Am. Chem. Soc.* **1976**, *98*, 5261.
(145) Crowder, G. A. *J. Mol. Struct.* **1971**, *10*, 290.

(146) Lu, R.; Gan, W.; Wu, B.-H.; Chen, H.; Wang, H.-F. *J. Phys. Chem. B* **2004**, *108*, 7297.
(147) Liu, D.; Ma, G.; Xu, M.; Allen, H. C. *Environ. Sci. Technol.* **2005**, *39*, 206.
(148) Xu, M.; Liu, D.; Allen, H. C. *Environ. Sci. Technol.* **2006**, *40*, 1566.
(149) Schmeltzer, J. M.; Porter, L. A.; Stewart, M. P.; Buriak, J. M. *Langmuir* **2002**, *18*, 2971.
(150) Love, J. C.; Estroff, L. A.; Kriebel, J. K.; Nuzzo, R. G.; Whitesides, G. M. *Chem. Rev.* **2005**, *105*, 1103.
(151) Pauling, L. The Nature of the Chemical Bond and the Structure of Molecules and Crystals; An Introduction to Modern Structural Chemistry, 3rd. ed.; Cornell University Press: Ithaca, NY, 1960.

JP803277S